Atmos. Meas. Tech. Discuss., 6, 3765–3818, 2013
www.atmos-meas-tech-discuss.net/6/3765/2013/
doi:10.5194/amtd-6-3765-2013

Atmospheric Measurement Techniques Discussions

Validation and empirical correction of MODIS AOT and AE over ocean

N. A. J. Schutgens[1], **M. Nakata**[2], **and T. Nakajima**[3]

[1]Atmospheric, Oceanic and Planetary Physics, University of Oxford, UK
[2]Faculty of Applied Sociology, Environmental Studies,Kinki university, Japan
[3]Atmospheric and Oceanic Research Institute, University of Tokyo, Japan

Received: 8 March 2013 – Accepted: 14 March 2013 – Published: 15 April 2013

Correspondence to: N. A. J. Schutgens (schutgens@physics.ox.ac.uk)

Published by Copernicus Publications on behalf of the European Geosciences Union.

Abstract

We present a validation study of Coll. 5 MODIS level 2 Aqua and Terra AOT and AE over ocean by comparison to coastal and island AERONET sites for the years 2003–2009. We show that MODIS AOT exhibits significant biases due to windspeed and cloudiness of the observed scene, while MODIS AE although overall unbiased, exhibits less spatial contrast on global scales than the AERONET observations. The same behaviour can be seen when MODIS AOT is compared against marine AERONET data, suggesting that the spatial coverage of our datasets does not preclude global conclusions. Thus, we develop empirical correction formulae for MODIS AOT and AE that signifcantly improve agreement of MODIS and AERONET observations. We show these correction formulae to be robust. Finally, we study random errors in the corrected MODIS AOT and AE and show that they mainly depend on AOT itself, although small contributions are present due to windspeed and cloud-fraction in AOT random errors and due to Ångström exponent and cloud fraction in AE random errors. Our analysis yields significantly higher random AOT errors than the official MODIS error estimate ($0.03 + 0.05\tau$), while random AE errors are smaller than might be expected. This new dataset of bias-corrected MODIS AOT and AE over ocean is intended for aerosol model validation and assimilation studies, but also has consequences as a stand-alone observational product. For instance, the corrected dataset suggests that much less fine mode aerosol is transported across the Pacific and Atlantic oceans.

1 Introduction

Aerosols affect the Earth's radiation budget, either through scattering and absorption of direct sunlight or through modification of cloud parameters. At the moment, aerosols are considered the dominant uncertainty in radiative forcing estimates for the Earth's atmosphere. They are especially interesting because their general impact seems to be

AMTD
6, 3765–3818, 2013

a cooling of the atmosphere and because they may actually slow-down warming by greenhouse gases on regional scales.

To increase our understanding of the aerosol system, major efforts to observe it have been launched in the past two decades. Although our most reliable observations come from ground-based observing networks (e.g. the AERONET sun photometers), substantial spatial coverage can only be achieved through satellite observations. One of the best known satellite datasets of aerosol observations are formed by the observations of the two MODIS sensors aboard the Aqua (local equator crossing time 13:30 LT) and Terra (local equator crossing time 10:30 LT) satellites, both part of the A-train constellation. These sensors fly at an altitude of 705 km and have a cross track view of 2330 km. They observe the earth in 36 different spectral bands, of which several bands in the visual and near-infrared are suited to aerosol retrievals.

The MODIS observations of aerosol are based on look-up tables that allow retrieval of multi-wavelength AOT from measured radiances (Tanre et al., 1997). To produce these look-up tables, assumptions on e.g. surface reflection and aerosol chemical composition are made. The observations have been validated through comparison with the AERONET ground-based network observations (Ichoku et al., 2002, 2005a; Remer et al., 2002; Remer et al., 2005; Remer et al., 2008; Bréon et al., 2011). For a comparison to the Marine AERONET data, see Smirnov et al. (2011); Adames et al. (2011). The main conclusion from these papers is that MODIS level 2 AOT over ocean shows significant agreement with AERONET observations.

There have also been attempts to compare MODIS to other satellite data, for instance Liu and Pinker (2008); Mishchenko et al. (2009, 2010) who compared MODIS and MISR AOT.

MODIS observations contain biases dependent on the observed scene. For instance, under cloudy conditions or when windspeeds are high, MODIS will systematically overestimate AOT over ocean compared to AERONET (Zhang and Reid, 2006; Shi et al., 2011). Quantification and, hopefully, correction of these biases is important for data assimilation purposes, where unbiased observations are used to "nudge" a model closer

AMTD
6, 3765–3818, 2013

to the observed atmospheric state. In addition to assimilation, unbiased observations serve an obvious purpose in validation efforts of aerosol transport models.

Zhang and Reid (2006) and Shi et al. (2011) developed empirical correction formulae for MODIS AOT over ocean through systematic comparison with AERONET observations. These formulae use supplementary data on surface wind fields, cloud coverage and aerosol fine mode fraction. The significantly more complex behaviour of surface albedo over land probably precludes development of correction formulae, but Hyer et al. (2011) have developed additional screening procedures that substantially reduce erroneous AOT observations over land.

Previous efforts at validating MODIS observations and correcting biases have focused on AOT. However, AE contains a lot of useful information on the aerosol system as it typically tracks particle size. Even though this interpretation may be ambiguous in the case of multi-modal aerosol size distributions, the use of observation operators (functions that map atmospheric distributions of aerosol to observables like AOT or AE) allows meaningful application of AE observations in the context of either assimilation or model validation. The advantage of AE over AOT at a second wavelength is that its formulation potentially allows for error balancing and decorrelation with AOT at 550 nm. This is not necessarily true for e.g. the so-called fine mode fraction.

In this paper, we validate Coll. 5 MODIS level 2 AOT and AE observations against AERONET and marine AERONET. Given the very similar results, we conclude that AERONET sampling does not substantially influence the validation of MODIS observations. Thus, we develop correction formulae for MODIS AOT and AE by regressing MODIS observations against AERONET observations. For the corrected MODIS AOT and AE, we develop simple models that describe the remaining random errors. In Table 1, we present the major differences between our analysis and the analyses by Zhang and Reid (2006) and Shi et al. (2011). The main differences are that we take great care to create a dataset of independent MODIS vs AERONET observations and include modis AE observations as well. We also compare MODIS AOT observations against Marine AERONET.

AMTD
6, 3765–3818, 2013

In Sect. 2, we introduce the three datasets that we will use in our analysis. Section 3 describes how we select the co-located MODIS-AERONET observations that will be used for validation of the original MODIS product (Sect. 4.1). The results of Sect. 4.1 will be corroborated by comparing the MODIS observations against Marine AERONET in Sect. 4.2. In Sect. 5, we explain how one may derive correction formulae for both MODIS AOT and AE. The robustness of that correction is also discussed. The global impact of our correction on AOT and AE observations over ocean is shown in Sect. 6, while the remaining random errors in AOT and AE are discussed in Sect. 7.

In this paper, we will call the deviation between co-located MODIS and AERONET AOT the MODIS AOT error. We assume that AERONET represents the truth or at least that its errors are negligible compared to MODIS. When dealing with a sample of co-located MODIS and AERONET observations, the median error will be called *bias* and half the interquantile range (15.8–84.2 %) will be called the *random error* of MODIS (note that this is the standard deviation in case of a Gaussian distribution).

Several figures in the paper show box-whisker plots that use a common interpretation. First, the sample was binned according to the variable on the horizontal axis. Per bin, the 10, 25, 50, 75 and 90 % quantiles of the MODIS error were determined. The open vertical bar shows the interquartile range (25–75 %) and the vertical lines extending from this open bar the 10 to 90 % interquantile range. The median is shown by the horizontal line inside the open bar. This median is surrounded by a solid bar (narrower than the open bar) that gives the 5 to 95 % interquantile range of median estimates according to a bootstrap analysis. Finally, over each bar a numerical value gives the number of observations per bin, either in counts (integers) or percentages (decimals).

2 MODIS, AERONET and NCEP-DOE-II data

We will use the following datasets: Coll. 5 MODIS Aqua and Terra Level 2 data, AERONET lev 2.0 from the direct sun algorithm, maritime AERONET lev 2.0 and NCEP-DOE-II 6-hourly reanalysis of windspeeds, temperature and specific humidity.

AMTD
6, 3765–3818, 2013

Data from 2003 (2004 for maritime AERONET) up to and including 2009 were downloaded from their respective websites.

The MODIS Coll. 5 level 2 data were downloaded from http://modis.gsfc.nasa.gov/. We will use the "average ocean" AOT product at 470, 550 and 860 nm (Remer et al., 2005). AOT at 470 and 860 nm is converted into an Ångtström exponent (AE) through:

$$\alpha = -\frac{\log\ \tau_2/\tau_1}{\log\ \lambda_2/\lambda_1}, \quad (1)$$

where τ and λ represent AOT and wavelength as usual. In addition, we will use supplementary data provided in the MODIS data product such as the observed cloud-fraction and the various scattering geometry angles (viewing zenith angle, solar zenith angle, etc.). All data over ocean irrespective of QA flag will be used as recommended by Remer et al. (2005) (see also Mishchenko et al., 2010). The MODIS AOT random error over ocean is often taken to be

$$\Delta\tau = 0.03 + 0.05\tau, \quad (2)$$

see e.g. Remer et al. (2005).

AERONET data (Holben et al., 1998) were downloaded from http://aeronet.gsfc.nasa.gov/ and are AOT at various wavelengths (440, 550, 675 and 870) derived from the direct sun algorithm. These AOT are converted into AOT at 550 nm (if not directly observed) and AE for 870/440 nm (using Eq. 1) for later comparison to MODIS. AERONET AOT errors are estimated to be ~ 0.01 (Eck et al., 1999; Schmid et al., 1999) and we will use AERONET as a reference to which MODIS may be compared. Not all AERONET sites, however, will be used as some may be less representative than others for comparison to MODIS satellite observations (see Sect. 5.1 for details). Allthough AERONET low level cloud screening is probably very good, there remain issues with cirrus clouds (Huang et al., 2011). All AERONET observations were averaged over 1 h, every hour.

AMTD
6, 3765–3818, 2013

Maritime AERONET data (Smirnov et al., 2011) were downloaded from http://aeronet.gsfc.nasa.gov/. Smirnov et al. estimate AOT errors to be ~0.02. No further screening was applied to these data, as they were only used for additional verification.

The NCEP-DOE-II reanalysis data (http://esrl.noaa.gov/) are the 6-hourly values for surface pressure, air temperature at 2 m, specific humidty at 2 m as well as windspeeds at 10 m at a global Gaussian T62 grid. This reanalysis is an improved version of the original NCEP reanalysis (Kalnay et al., 1996). The NCEP-DOE-II data were linearly interpolated to the location and time of the MODIS pixel.

3 MODIS data screening

3.1 Common sense quality control criteria

We will start by screening the complete MODIS observational dataset using the same rules of thumb that Zhang and Reid (2006) proposed and Shi et al. (2011) used. We will discard any observation with AOT > 3, as radiances tend to saturate beyond this value (? % of data is lost). We will also discard any observation with a cloud fraction larger than 0.8 (? % of data is discarded). Zhang and Reid (2006) found increased differences between MODIS and AERONET AOT for large cloud fractions and (Liu and Pinker, 2008) found significant less correlation among MODIS and MISR AOT for cloud fractions above 0.8. We also discard any observation that is isolated, i.e. does not have at least one neighbour (? % of data is discarded). Finally, we discard observations hat show too much spatial variation (defined as the standard deviation across a set of 3 by 3 MODIS pixels). Our hope is that the latter two criteria will eliminate the worst cases of cloud-contaminated observations but undoubtably good observations with strong spatial AOT gradients will be removed as well. A typical standard deviation across a 3 by 3 MODIS pixel is determined as a function of AOT. Typically, this standard deviation increases as AOT increases (see Fig. 8 in Zhang and Reid, 2006, or Fig. 2 in Shi et al., 2011). By discarding those pixels that have a standard deviation larger than 1 times

AMTD
6, 3765–3818, 2013

the typical value, we remove the pixels with the strongest spatial gradients (% of data). Note that Zhang and Reid (2006) and Shi et al. (2011) use 1.5 times the typical value as criterium. Zhang and Reid (2006) and Shi et al. (2011) allowed some observations observed within the sun glint angle $\theta > 30^{\circ}$, but we only allow pixels outside the glint angle ($\theta > 40^{\circ}$).

3.2 Co-location of MODIS and AERONET observations

After screening the MODIS observations in the manner described above, we co-locate them with AERONET observations. Any MODIS observation within 50 km and within 30 min of an AERONET observation (1 h averages, see Sect. 2) is considered co-located. We varied these criteria within reasonable bounds and concluded that, for the above values, correlation among MODIS and AERONET AOT at 550 nm is maximal. This agrees well with other studies (Ichoku et al., 2002; Bréon et al., 2011). Because of this co-location criterium, several individual MODIS observations will be co-located with the same AERONET observation. On average, every AERONET observation is co-located with 10 MODIS observations, although the actual number varies between 1 and 76.

3.3 Apparent biases due to the co-location criterium

In any spatio-temporal field of bounded measurements, large values are more likely to be surrounded (in a spatio-temporal sense) by lower values and vice-versa. This would lead to *apparent* biases of even an ideal (error-less) dataset against another ideal (error-less) dataset. Figure 2 shows such apparent bias. Here both datasets come from a time-series of AERONET AOT, one from the original time-series and the other from the time-series shifted by either 1 or 6 h. Although large negative biases are obvious for a 6 h separation, they are strongly reduced for a 1 h separation. Note that using the correlation between MODIS and AERONET to optimise co-location criteria does

AMTD
6, 3765–3818, 2013

not automatically exclude cases where these apparent biases are strong, but given our short time separations (less than 30 min), this effect will not influence our analysis.

3.4 Spatial correlations in MODIS observations

Observed aerosol fields are known to exhibit correlations over tens of kilometers (Anderson et al., 2003; Kovacs, 2006; Santese et al., 2007), due to the nature of transport of aerosol particles. We expect to see such long correlation lengthscales in our MODIS data-set, especially since our common sense quality control criteria preferentially select homogeneous scenes. Furthermore, spatial correlations are likely to exist in MODIS errors as retrieval assumptions (e.g. surface albedo, atmospheric water vapour content, particle models) exhibit spatial correlations. In Fig. 1, we show the spatial correlations in both the MODIS observations and their errors. From all co-located MODIS observations at each AERONET site and time, pairs of MODIS observations at different spatial separations were randomly chosen. For each separation bin, a correlation was then computed over all eligible pairs for all sites and times. As we constrained our co-located observations to a distance of 50 km from the AERONET site, the spatial separation of these MODIS pixels can never be more than 142 km, but in our sample is never more than 100 km. We see that MODIS observations themselves show strong correlations over these 100 km. The spatial correlations in MODIS errors are lower than those in AOT itself but still very substantial. As a matter of fact, both the MODIS observations and their errors within a 50 × 50 km gridbox (∼ 0.5 × 0.5° at the equator) are strongly correlated.

3.5 Independent sub-samples of MODIS observations

In principle, a statistical analysis of any dataset is best conducted on an independent sample, although data scarcity may make this difficult. If one uses all co-located MODIS observations in the analysis, the sample is *not* independent. One reason is that many MODIS observations will be compared against the same AERONET observation.

AMTD
6, 3765–3818, 2013

Another reason is that the MODIS observations themselves are spatially correlated. To obtain an independent sample, one only needs to sub-sample modis observations by choosing a single observations for each AERONET site and each time. Different strategies exist for choosing this single MODIS observation, although the observation closest to the AERONET observations seems the most logical. Figure 3 shows the MODIS AOT error as a function of MODIS AOT using either all observations or a independent sub-sample of observations. We see that the sub-sample leads to larger biases, or conversely, that correlations in the full dataset will suppress the biases. Another example is shown in Fig. 4 where various sampling strategies are used to determine the MODIS AOT error for $0.5 < \mathrm{AOT} < 1.5$. When sub-sampling only the *closest* or *farthest* MODIS observation, markedly larger biases are found than for the full data-set (all) or a random sub-sample of the full dataset (random). The reason becomes clear if we create independent sub-samples of only clear or cloudy MODIS pixels. Cloud-free scenes allow more succesful retrievals (more co-located pixels) than cloudy scenes. When using the full data-set, one biases the MODIS errors in favour of cloud-free scenes. Similarly, we find that independent sub-samples shows lower MODIS bias at large windspeeds ($> 16\,\mathrm{m\,s^{-1}}$) than the full data-set (not shown). Hence it is important to perform the following error analysis with an independent sub-sample. We will return to the impact of different sampling strategies on MODIS errors later (in Sects. 5.3 and 5.4).

4 Validation of MODIS AOT and AE

4.1 Comparison against AERONET

In the following, we will use the independent sub-sample based on the closest MODIS observation to any AERONET observation. We will now study how AOT and AE error statistics change as a number of important parameters change. These parameters include AERONET AOT and AE, the MODIS scattering geometry angles as well as

AMTD
6, 3765–3818, 2013

environmental variables such as windspeed, cloud fraction, temperature and relative humidity.

Figure 5 shows the main four parameters that affect MODIS AOT error statistics, both its biases and its random errors. They are AERONET AOT and AE themselves, windspeed and cloud-fraction. We see that MODIS biases increase with windspeed and cloud fraction but decrease with AOT and AE. The influence of windspeed and cloud fraction on MODIS AOT bias is well-known and due to limitations in the Collection 5 retrieval algorithms. The co-variation of the bias in AOT with AE suggest that there are still issues with the assumed scattering properties of the MODIS aerosol types. Note that random errors depend mainly on AOT.

Glint angles, at least down to 40°, (Fig. 6) have almost no influence on error statistics, in contrast to what was reported by Zhang and Reid (2006) and Shi et al. (2011) (who allowed glint angles down to 30°). Like Ichoku et al. (2005a), we do not see a clear dependence on scattering angles (see also Mishchenko et al. (2009) who compares MODIS AOT to MISR). We do see, however, a significantly higher bias for SZA $< 20°$. Similarly, we see significantly higher biases for temperatures $T < 260$ K and relative humidities RH < 0.2. These high biases are robust when we use different sub samples and occur only at a small number of sites, for only a few MODIS observations at each site. The bias for low temperatures may be an issue with the NCEP-DOE-II reanalysis as it only occurs for a few sites on the east coast of north America. For Aqua, there is a substantial overlap between the cases with low relative humidity and low solar zenith angle, but not so for Terra.

We also found, unsurprisingly, that MODIS AOT biases increase significantly with altitude of the AERONET site (not shown). For AERONET altitudes above 300 m (on mountains near the coast or on islands), the collocated MODIS observed air column (over ocean) and AERONET observed air column differ substantially and the AERONET site can not be considered representative for the MODIS observation.

Figure 7 shows the error statistics of MODIS AE. AERONET AE has a strong impact on AE biases with AE error positively biased for low AERONET AE and negatively

AMTD
6, 3765–3818, 2013

biased for high AE. As a result, MODIS AE has no significant bias as a whole but shows reduced contrast in space or time compared to AERONET. There is also a negative bias for large windspeeds. Balancing of errors in AOT (see Eq. 1) is probably the reason that AE bias hardly depends on AOT, cloud fraction or any other parameter. The random AE error depends strongly on AOT.

Finally, we point out that several of the discussed parameters co-vary to a certain extent. Obviously, this is the case for the scattering angles. But there is also a weak correlation between e.g. cloud fraction and windspeed, maybe because whitecaps are interpreted as cloudiness.

4.2 Comparison against Marine AERONET

Marine AERONET data has a substantially different spatial sampling than AERONET. Not only does Marine AERONET contain many observations over the deep ocean, but is also better balanced as regards the latitudinal distribution of observations (the majority of AERONET observations are made in the Northern Hemisphere). Here we will show that MODIS Terra AOT shows very similar biases versus marine AERONET as against the regular AERONET data.

Figure 21 shows biases in Terra against both AERONET and marine AERONET for either the full dataset or an independent dataset. For the latter, there clearly is a large similarity between the AERONET and Marine AERONETcomparison When using the full dataset, Marine AERONET data suggest MODIS Terra AOT errors are systematically 0.01 to 0.02 lower than AERONET data suggest. Note that the independent dataset with Marine AERONET observations are small: only 395 (Aqua) or 426 (Terra) data pairs are available. Similar results can be shown for æ biases in MODIS Terra although the picture is noisier (the data set is even smaller: 283).

The comparison with Aqua yields ambiguous results. In particular, the bias in MODIS Aqua AOT vs. marine AERONET shows no dependency on either AE or cloud-fraction. Since this dependency has been shown to exist for MODIS Aqua against AERONET (see Zhang and Reid, 2006; Shi et al., 2011; and Sect. 4.1) and MODIS Terra against

AMTD
6, 3765–3818, 2013

marine AERONET, this is a surprising result. What is causing this remarkable deviation from a clear pattern is far from obvious but also outside the scope of this paper.

Figure 21 seems to suggest there are differences in the random MODIS errors when using either AERONET or Marine AERONET data. However, Marine AERONET tend to have smaller AOT and AE observations than AERONET. We will later (Sect. 7) show that random MODIS errors depend strongly on AOT and weakly on AE. In particular, AERONET's median AOT is 0.119 while marine AERONET's median AOT is 0.077, 30 % lower. To make a meaningful comparison, Fig. 22 shows MODIS Terra random AOT errors estimated from either AERONET or Marine AERONET data as a function of AOT. It would appear the random errors estimated from AERONET data are somewhat larger than those estimated from Marine AERONET. However, if we subsample the AERONET data to a dataset that is close to Marine AERONET in terms of size, observed AOT, AE, windspeed and cloud fraction it turns out there is quite some variation in the estimated random error (dotted blue lines in the figure). It seems not possible to conclude from the current datasets that AERONET and Marine AERONET yield different random MODIS errors. Note that the Marine AERONET analysis has its own statistical uncertainty which is however difficult to assess due to its low sample size.

5 Empirical correction of MODIS AOT and AE

In this section, we will describe a new method for empirically correcting MODIS observations through regression onto the co-located AERONET observations. Before doing this, we will further screen MODIS data by removing all MODIS observations for $T < 260\,\mathrm{K}$, $\mathrm{RH} < 0.2$ or $\mathrm{SZA} < 20^{\circ}$. The previous section showed that MODIS AOT biases were unusually large for those parameter values. This leads to a further reduction in the sample size of our co-located observations of about 3 %.

AMTD
6, 3765–3818, 2013

5.1 Screening of AERONET sites

So far we have not really considered how appropriate the AERONET sites are for validation of MODIS observations. In the previous section we saw that AERONET sites at altitudes above 300 m generally show poorer agreement with MODIS data and this is likely due to the different air columns observed. Local emission sources or orography can similarly cause AERONET observations to not be representative of the larger area sampled by MODISBy studying the correlation between MODIS and AERONET AOT per site we will try to remove unrepresentative AERONET sites. Thus we calculate correlation coefficients and linear regression coefficients for the co-located MODIS and AERONET data per site. If the number of co-located data per site is below 11 we discard that particular site from our analysis. If the correlation coefficient is below 0.5 or the regression coefficient below 0.5 or above 2.0, we also discard that site, because seemingly these AERONET observations are not representative of the co-located MODIS observations. The total loss in co-located data is ∼4 %, with most due to minimum requirement for the number of observations. The number of discarded sites depends to some extent on the sensor and the chosen subsample, so this selection maybe too conservative (i.e. remove even good data). The sites that are consistently removed, independent of sensor or subsample, are: Adelaide_site_7, CEILAP-RG, Coconut Island, Crozet Island and REUNION_ST_DENIS. As these sites all have sufficient number of observations co-located with MODIS, even after our screening, we contacted their respective PI's, hoping to understand why there might be a big discrepancy between those sites and AERONET. Unfortunately, no obvious reasons could be found. Also, we include in our analysis several sites that (Ichoku et al., 2005b) excluded.

5.2 Methodology of the empirical correction

A correction of MODIS AOT and AE is now developed as a regression of the MODIS bias unto the predictors of this bias: AOT, AE, windspeed and cloud fraction. A correct regression faces several obstacles: the non-Gaussian distribution of the observations

AMTD
6, 3765–3818, 2013

(in particular, the strongly skewed distribution of AOT itself and the many outliers in the MODIS bias), the multiple parameters that influence the errors (see previous subsection) and the (weak) co-variation of some of these parameters. As robust multiple (linear) regression is a field very much in development and no standard techniques are yet available, we decided to pursue a common sense approach.

Looking at Fig. 5, it appears rather straightforward to develop corrections for the AOT bias due to windspeed and cloud fraction. For instance, the windspeed correction could be based on a linear regression of the bias unto windspeed. Similarly, a cloud fraction correction may be developed. If these corrections are developed independently, the combination of both corrections may actually yield a product that is less accurate than the standard product. Instead, one could first develop a correction for windspeed and then correct the windspeed-corrected (!) MODIS AOT for cloud fraction. Or the other way around: first correct for cloud fraction and then for windspeed. This does not automatically lead to an improved product, but there are now two correction algorithms that are different and hopefully at least one leads to MODIS AOT with significantly reduced biases overall.

In practice, we want to correct not only for windspeed and cloud fraction, but also AOT and AE. As AERONET AOT and AE are not available for the majority of MODIS observations, we will use their MODIS observed counterparts as proxies. As a possible MODIS correction algorithm, we now define any particular permutation of sequential correction by AOT, AE, windspeed and cloud fraction (4! = 24 algorithms). The corrections due to AE, windspeed and cloud fraction can either be added to or multiplied with the MODIS AOT ($2^3 \cdot 24 = 192$ algorithms). Finally, the AOT bias as a function of AOT seems to exhibit to regimes: constant for small AOT and a linear dependence for larger AOT (not shown). We therefor develop correction algorithms, one for low and one for high AOT. Furthermore, we will optimize the threshold AOT value for using either algorithm by attempting 5 different values (Zhang and Reid (2006) and Shi et al. (2011) assumed a threshold of 0.2). All in all, we developed 960 different algorithms per AOT regime, and then chose the optimal algorithm.

AMTD
6, 3765–3818, 2013

The actual regression of the MODIS bias unto a single parameter, say cloud-fraction, is performed as follows. First we divide the cloud-fraction data in 4 bins with equal number of observations. For each bin, a median cloud-fraction, median MODIS error (i.e. the bias for that bin) and an error estimate in the later are determined. The linear regression for these values constitutes one particular correction formula.

The optimal algorithm is a sequence of correction formula that minimizes the MODIS bias the most. Since there is a substantial contribution from random errors in the MODIS data, a special metric was used to assess that reduction. First, we divide the (corrected) MODIS data in four bins of equal numbers of AOT observations (or AE). For each AOT bin separate regressions of MODIS error vs AOT, AE, windspeed or cloud-fraction are made. The RMS value of the *regression* against e.g. windspeed we call the bias due to the windspeed for that particular AOT bin (note this RMS value will be zero in the absence of biases). The errors for all four AOT bins are now averaged to yield a typical MODIS bias for windspeed. These biases are further averaged for all four parameters AOT,AE, windspeed and cloud-fraction to yield a single metric (henceforth simply called bias). Note that this is a very different value from e.g. the RMS difference of MODIS and AERONET AOT, as there the latter will be dominated by substantial random noise. The bias will be used to compare algorithms. In practice, various algorithms will perform similarly good or bad and it is not possible to single out any algorithm as *the* optimal algorithm. This is not necessary anyway. What is important is that there are algorithms that substantially reduce the bias, while others fail and may even increase it.

5.3 Results for MODIS AOT

We can reduce the bias metric for AOT by a factor of ~ 3. In the case of Terra, it is useful to also include a correction based on scattering angle. The optimal correction algorithms are presented in Appendix A.

For Aqua, the bias metric is reduced from 0.018 to 0.007. Figure 8 shows how the biases change as a function of AOT, AE, windspeed and cloud fraction. Clearly, Aqua

AMTD
6, 3765–3818, 2013

random errors hardly change (resp. 0.076 and 0.077). Correlation coefficient for all MODIS-AERONET AOT pairs also barely changes, from 0.86 to 0.87, but the coefficient of a robust linear regression experiences a significant increase (from 0.89 to 0.99). A density plot (Fig. 9) of Aqua AOT vs. AERONET AOT shows a striking improvement in the agreement with AERONET at low AOT. Not only do we see an improvement in the whole sub-sample but also at individual AERONET sites. E.g. the median of the linear regression coefficients per AERONET site changes from 0.90 to 1.00. Due to the correction, the median value of Aqua AOT changes by −0.013, with 25 % of the data experiencing a reduction of more than 29 %.

For Terra, the bias metric is reduced from 0.018 to 0.006. Neither the Terra random error (from 0.078 to 0.079) nor the correlation hardly change (from 0.87 to 0.89). A robust linear regression over all MODIS-AERONET data pairs sees a small increase in the coefficient (from 0.95 to 1.00). The median of the regression coefficients per AERONET site changes from 0.97 to 1.01. In the case of Terra, the median value of AOT changes by −0.022, with 25 % of the data experiencing a reduction of more than 36 % due to this correction.

The correction algorithm is robust. In Fig. 10, we show remaining biases in Aqua observations when the correction algorithm from Appendix A is applied to different subsamples (random or the farthest co-located pixel) as well as the full dataset. We see that the full dataset sometimes shows very different biases from the subsets whose biases are closer together.

For Terra, similar results can be shown.

As a last independent test, we applied the correction algorithm to data for 2011 and 2012. Inspection of graphics as shown in this section, show that also for this time period the correction formula work well. Since there is less data, results are noisier but over all biases are reduced (from 0.028 to 0.009) and the regression coefficient is slightly improved (0.87 to 0.87) for Terra AOT. For Aqua, biases remain the same (0.018 and 0.017) for and the regression coefficient increases from 0.76 to 0.84. Sample sizes are less than 2000.

AMTD
6, 3765–3818, 2013

5.4 Results for MODIS AE

Before we discuss the correction of MODIS AE, we will study MODIS AE derived from Eq. (1) further. Errors in AE are determined by errors in AOT so we wonder how well MODIS and AERONET AE agree depending on MODIS AOT. Usually $\tau_{470} > \tau_{860}$ and AOT at 860 nm is the more error prone value (due to surface reflection or cloud contamination). In Fig. 11, we show the correlation and bias of MODIS AE with respect to AERONET AE for AOT bins with equal number of observations (> 15 000 as we use the full dataset, but results are very similar for any independent sub-sample). For low AOT at 860 nm, correlations are small and biases are large which suggests it would be difficult to develop correction algorithms. When one inspects scatter plots for individual AOT bins, one sees that for low AOT, MODIS often has AE > 2. In particular there appears to be a peak in the AE histogram for AE ∼ 2.7. We therefor choose minimum threshholds ($\tau_{860} > 0.055$) for MODIS τ_{860} before we continue our analysis (resulting in a loss of 31 % of AE data).

The correction of AE proceeds in the same way as that of AOT. We can reduce the bias metric for in AE by a factor of 2. The correction includes influences from AE, windspeed and scattering angle. The optimal correction algorithms are presented in Appendix A.

For Aqua AE, the bias metric is reduced from 0.09 to 0.046, but the component due to AE is reduced from 0.24 to 0.07. Figure 12 shows how these biases change as a function of AOT, AE, windspeed and cloud fraction. As a consequence of the bias correction, random errors increase from 0.40 to 0.54 (a consequence of the rescaling of AE). The correlation coefficient between MODIS and AERONET AE changes not (0.69) but the linear regression coefficient changes significantly from 0.58 to 0.94. A density plot (Fig. 13) of Aqua AE vs. AERONET AE shows a striking improvement in the agreement with AERONET. The median of regression coefficient per AERONET site changes from 0.53 to 0.86.

AMTD
6, 3765–3818, 2013

For Terra AE, the bias metric is reduced from 0.12 to 0.07 while component due to AE is reduced from 0.24 to 0.11. As a consequence of the bias correction, random errors increase from 0.41 to 0.51. Again, the correlation coefficient does not change (0.69) but the robust linear regression coefficient changes from 0.63 to 0.94. The median of the regression coefficients per station changes from 0.58 to 0.83.

As was the case for AOT biases, the AE correction scheme is robust. In Fig. 14, we show remaining biases in Aqua observations when the correction algorithm is applied to different subsamples (random or the farthest co-located pixel) as well as the full dataset.

For Terra, similar results can be shown.

As a last independent test, we applied the correction algorithm to data for 2011 and 2012. Inspection of graphics as shown in this section, show that also for this time period the correction formula work well. Since there is less data, results are noisier but over all biases are reduced (from −0.1 to −0.02) and the regression coefficient is improved (0.55 to 0.75) for Terra AE. For Aqua, biases increase for −0.027 to 0.028 and the regression coefficient increases from 0.56 to 0.91. Sample sizes are less than 2000.

6 Multi-year averages of MODIS AOT and AE

In this section, we will show the impact of the corrections on the 2003-2009 averages of MODIS Aqua AOT and AE. We will show figures of the original MODIS Coll. 5 lvl 2 product, the screened product (Sect. 3) and the corrected product (Sect. 5). Only MODIS Aqua will be considered here, Terra shows very similar results. These multi-year averages should not be taken as climatologies, as we have not made any effort to homogenize spatial and temporal sampling. In particular, the original and the screened product differ simply because many observations are discarded. The screened and corrected product have, however, the same spatial and temporal sampling.

In Fig. 15 we show MODIS Aqua AOT. Both the screening and correction lead to substantial changes in AOT distribution. In particular over cloudy regions, more

AMTD
6, 3765–3818, 2013

observations are discarded and those that remain undergo larger corrections (e.g. at mid-latitudes in both hemispheres). The correction strongly reduces spatial variation in AOT. Note there is nothing in the correction algorithm that produces such a result a priori. Continental outflows extend less far across the oceans and the elevated band of AOT at southern mid-latitudes has mostly disappeared.

In Fig. 16 we show MODIS Aqua AE. Again, both the screening and the corrections lead to significant changes in AE. The screening removes very high AE values at high latitudes, while the correction increases AE close to land and decreases it for the middle of the ocean. As a consequence, land-ocean and north-south gradients become more pronounced. Due to the correction, regional detail increases: there is more contrast between the dust and carbon outflows on the Western coast of Africa, and between Indian (pollution) and Arabian (dust) outflows.

7 Random errors in MODIS AOT and AE

In this section, we will address the random errors in the corrected MODIS AOT and AE. In Figs. 8 and 12, we indicated this error as the interquartile range for various AOT, AE, windspeed and cloud fraction bins. Both the AOT and AE random error depend on AOT itself, but there appear to be correlations with other parameters as well. This random error is usually expressed as the standard deviation of a distribution of errors, but we will use half the quantile range from 15.8 to 84.2 %. Since our error distributions generally have narrower peaks and wider wings than Gaussian distributions and may also be skewed, quantiles seem a more appropriate measure as the common standard deviation tends to overestimate the width of the distribution. In Fig. 17 we show actual Aqua AOT error distributions per AERONET AOT bin, as well distributions based on either the standard deviation or our proposed interquantile range. Especially for low and high AOT, a Gaussian distribution based on an interquantile range appears the better choice.

AMTD
6, 3765–3818, 2013

We now present simple models for the random errors based on the assumption that the various error sources are independent. These models were built in a trial and error manner. In the case of AOT random errors, for instance, we first considered only observations for low cloudiness and windspeed. For those observations, a function in AOT was sought that well described the random errors. Next, all observations were considered and small corrections due to windspeed and cloud fraction were added.

Figure 18 shows the random errors in AOT for Aqua as a function of binned AOT, AE, windspeed or cloud fraction by estimating standard deviations per bin. We also show the estimate from our simple model (see also Appendix A), which agrees quite nicely. Note that the variation in AOT random error with AE is mostly due to the sampling of AOT values (low AE often implies high AOT).

The random error in AE as a function of binned AOT, AE, windspeed or cloud fraction is shown in Fig. 19. Again, our simple error model agrees nicely. As expected, AOT has a huge impact on AE random error, but its variation with AE cannot be solely understood due to AOT sampling alone (i.e. AE influences the AE random error, with larger AE having a larger random error).

Finally, we compare the above random error models with those found in previous papers. We will limit ourselves to the AOT dependency only. In the top panel of Fig. 20, random AOT errors are shown. The estimate by Remer et al. (2005) is clearly lower than estimates by Zhang and Reid (2006); Shi et al. (2011) and this study. The latter studies agree in a general way but we find larger errors for large AOT. In the bottom panel of the same figure, AE random errors are shown. In dashed lines, AE errors predicted from AOT errors are shown. In that prediction we assumed identical but uncorrelated errors at the two wavelengths, in which case (see also Eq. 1),

$$\Delta\alpha = \frac{\sqrt{1/\tau_1^2 + 1/\tau_2^2}}{\log\lambda_2/\lambda_1}\Delta\tau \quad (3)$$

As the actual random AE errors (solid line) are often lower (even lower than AE errors estimated from Remer et al., 2005, AOT errors), it would appear that substantial

AMTD
6, 3765–3818, 2013

correlations in AOT errors at different wavelengths reduce AE random errors, just as we hoped.

8 Conclusions

We have validated Coll. 5 MODIS level 2 AOT and AE observations over ocean against collocated AERONET and Marine AERONET observations. Based on this study, we propose additional quality control selection criteria and empirical correction algorithms to construct a smaller subset of MODIS observations that agree optimally with AERONET. This subset has similar spatial and temporal coverage as the full MODIS dataset but greatly reduced biases. Random errors of the corrected observations are also evaluated and error models developed. Random AOT errors for $\tau > 0.1$ are shown to be larger than the error estimate often used ($0.03 + 0.05\tau$). Random AE errors are shown to be *smaller* than might be expected.

Our work is both an extension and an improvement of work done by Zhang and Reid (2006) and Shi et al. (2011). The extension consists of an analysis of MODIS AE observations over ocean and greater detail in the behaviour of MODIS biases and random errors as well as corroborative evidence from Marine AERONET. The improvement is in a different statistical approach (using independent samples) and a different construction of the correction algorithm (that allows optimisation of not only its parameters but also its structural form). We also use a different reanalysis dataset (NCEP-DOE-II) to obtain auxiliary data like wind speeds.

To our knowledge, this is the first paper to compare MODIS AE observations against an independent dataset. We show that there is a useful signal in MODIS AE after proper screening (including a minimum value threshold on associated τ_{860}). Although MODIS fine mode AOT is sometimes used by researchers, no error analysis is available for this product. We provide a full error analysis (bias and random errors) for MODIS AE, which serves a similar role as fine mode AOT (separation of coarse and fine mode aerosol).

AMTD
6, 3765–3818, 2013

Like Zhang and Reid (2006) and Shi et al. (2011) and other authors we note the increase in MODIS AOT bias with increasing windspeed or cloud fraction. This is probably due to incorrect assumptions for the surface albedo. We note that in Coll. 6, steps have been taken to represent more different sea states. MODIS AE biases depend mostly on AE itself, suggesting issues with the aerosol scattering models used in the retrieval. This is also suggested by a random error in AOT that increases with AOT.

As a result of our corrections, MODIS AOT reduces by at least 30 % for 25 % of the observations and the elevated AOT over the Southern ocean have mostly disappeared. MODIS AE decreases by at least 0.2 for 25 % of the observations and increases by at least 0.2 for another 25 % of the observations, leading to increased AE contrasts between the Northern and Southern hemipsheres and between coastal areas and the open ocean.

The bias-corrected MODIS over ocean AOT and AE observations can be used for model validation or data assimilation. Our own interest is in the estimation of aerosol emissions from remote sensing observations (Schutgens et al., 2012). This bias correction also has consequences for the global aerosol distribution. Global maps of multi-year averaged bias-corrected AOT and AE show that far less fine mode particles are transported across the oceans than the original MODIS product suggests.

Appendix A

MODIS AOT and AE selection and correction

A1 Data selection for MODIS AOT and AE

- Discard any MODIS pixel with original $\tau_{550} > 3$.
- Discard any MODIS pixel with cloud fraction > 0.8.
- Discard any MODIS pixel that has no neighbours.

AMTD
6, 3765–3818, 2013

- Discard any MODIS pixel whose standard error is larger than:
  - Terra: $0.003 + 0.036\tau_{550} + 0.023\tau_{550}^2$.
  - Aqua: $0.002 + 0.040\tau_{550} + 0.021\tau_{550}^2$.
- Discard any MODIS pixel with SZA$< 20^\circ$.
- Discard any MODIS pixel for which RH < 0.2 and $T < 260$ K.

A2 Correction for MODIS AOT

The following equations should be processed sequentially, like FORTRAN computer code.

If Terra $\tau_{550} \leq 0.049$ then

$$\tau_{550} = (1 + 0.181581 - 0.0168456w)\tau_{550} \quad \text{(A1)}$$

$$\tau_{550} = (\tau_{550} - 0.0287665)/0.243752 \quad \text{(A2)}$$

$$\tau_{550} = \tau_{550} + 0.0207946 - 0.000153499\Theta \quad \text{(A3)}$$

$$\tau_{550} = (1 - 0.364205 - 0.100776f_c)\tau_{550} \quad \text{(A4)}$$

$$\tau_{550} = (1.0 - 0.0822829 + 0.0781099\alpha)\tau_{550} \quad \text{(A5)}$$

If Terra $\tau_{550} > 0.049$ then

$$\tau_{550} = \tau_{550} - 0.0122103 - 0.0358403f_c \quad \text{(A6)}$$

$$\tau_{550} = \tau_{550} + 0.0320079 - 0.000243895\Theta \quad \text{(A7)}$$

$$\tau_{550} = \tau_{550} - 0.0294600 + 0.0266009\alpha \quad \text{(A8)}$$

$$\tau_{550} = (\tau_{550} - 0.0142035)/0.898996 \quad \text{(A9)}$$

$$\tau_{550} = \tau_{550} + 0.00378178 - 0.000665484w \quad \text{(A10)}$$

AMTD
6, 3765–3818, 2013

If Aqua $\tau_{550} \leq 0.05$ then

$$\tau_{550} = (1 + 0.315863 - 0.0306199w)\tau_{550} \quad \text{(A11)}$$

$$\tau_{550} = (\tau_{550} - 0.0271628)/0.301162 \quad \text{(A12)}$$

$$\tau_{550} = \tau_{550} + 0.00514700 - 0.0274383f_c \quad \text{(A13)}$$

$$\tau_{550} = (1 - 0.350973 + 0.0378387\alpha)\tau_{550} \quad \text{(A14)}$$

If Aqua $\tau_{550} > 0.05$ then

$$\tau_{550} = (1 - 0.258509 + 0.164087\alpha)\tau_{550} \quad \text{(A15)}$$

$$\tau_{550} = (\tau_{550} - 0.0328901)/0.760698 \quad \text{(A16)}$$

$$\tau_{550} = \tau_{550} + 0.00646153 - 0.0322341f_c \quad \text{(A17)}$$

$$\tau_{550} = \tau_{550} + 0.0106865 - 0.00186725w \quad \text{(A18)}$$

where α is the original MODIS AE, Θ the scattering angle, w the NCEP-DOE-II 2 m windspeed and f_c the cloud fraction.

A3 Additional selection criterium for AE

For AE we use an additional selection criterium that optimizes the agreement between the original MODIS and AERONET AE

- Aqua: $\tau_{860} \geq 0.055$.
- Terra: $\tau_{860} \geq 0.057$.

A4 Correction for MODIS AE

The following equations should be processed sequentially, like FORTRAN computer code.

AMTD
6, 3765–3818, 2013

If Terra $\tau_{550} \leq 0.083$ then

$$\alpha = \alpha + 0.239255 + 0.0181123w \quad \text{(A19)}$$

$$\alpha = (\alpha - 0.640555)/0.229146 \quad \text{(A20)}$$

$$\alpha = \alpha + 1.00041 - 0.00732544\Theta \quad \text{(A21)}$$

If Terra $\tau_{550} > 0.083$ then

$$\alpha = \alpha + 0.423368 - 0.00279822\Theta \quad \text{(A22)}$$

$$\alpha = (\alpha - 0.334271)/0.667072 \quad \text{(A23)}$$

$$\alpha = \alpha - 0.128672 + 0.0246823w \quad \text{(A24)}$$

If Aqua $\tau_{550} \leq 0.087$ then

$$\alpha = (\alpha - 0.404072)/0.278597 \quad \text{(A25)}$$

$$\alpha = (1.0 + 0.200161 - 0.00561571\Theta)\alpha \quad \text{(A26)}$$

$$\alpha = \alpha + 0.155928 + 0.0268758w \quad \text{(A27)}$$

If Aqua $\tau_{550} > 0.087$ then

$$\alpha = (\alpha - 0.429633)/0.586594 \quad \text{(A28)}$$

$$\alpha = \alpha - 0.166538 + 0.0317318w \quad \text{(A29)}$$

$$\alpha = \alpha + 0.101102 - 0.000775233\Theta \quad \text{(A30)}$$

AMTD
6, 3765–3818, 2013

A5 Random error in MODIS AOT

For Terra, the random error in AOT at 550 nm can be modelled with

$$\begin{aligned}\epsilon =& 0.045 - \tau e^{-\frac{\tau}{0.045}} + \\ & 0.24(\tau^2 - 0.045^2)(1 - e^{-\frac{\tau}{0.045}}) + \\ & 0.0125 f_c + \\ & \begin{cases} 0 & \text{if } w \le 8\ \mathrm{m\,s^{-1}} \\ 0.003(w - 8) & \text{if } w > 8\ \mathrm{m\,s^{-1}} \end{cases}\end{aligned} \tag{A31}$$

For Aqua, the random error in AOT at 550 nm can be modeleld with

$$\begin{aligned}\epsilon =& 0.0425 - 1.25\tau e^{-\frac{\tau}{0.0325}} + \\ & (0.25 \cdot (\tau^2 - .0325^2)) \cdot (1 - e^{-\frac{\tau}{0.0325}}) + \\ & 0.0125 f_c + \\ & \begin{cases} 0 & \text{if } w \le 8\ \mathrm{m\,s^{-1}} \\ 0.0035(w - 8) & \text{if } w > 8\ \mathrm{m\,s^{-1}} \end{cases}\end{aligned} \tag{A32}$$

A6 Random error in MODIS AE

For Terra, the random error in AE is reasonably well described by

$$\epsilon = 0.25 + 0.06\alpha + \exp\left(-3.75\sqrt{\tau_{550}}\right) \tag{A33}$$

For Aqua, the random error in AE is reasonably well described by

$$\epsilon = 0.25 + 0.08\alpha + \exp\left(-5\sqrt{\tau_{550}}\right) \tag{A34}$$

AMTD
6, 3765–3818, 2013

Acknowledgements. We thank the relevant PIs and their staff for establishing and maintaining the AERONET sites used in this investigation. The NASA MODIS team is acknowledged for preparing and making available MODIS observations. Part of this research was supported by funds from MOE/GOSAT, MOE/GER fund A1101, JST/CREST/EMS/TEEDDA, JAXA/EarthCARE and GCOM-C, MEXT/VL for climate diagnostics, MEXT/RECCA/SALSA, MEXT/KAKENHI/Innovative Areas 2409. The majority of this work was done while the first author was employed at AORI, University of Tokyo, Japan.

References

Adames, A. F., Reynolds, M., Smirnov, A., Covert, D. S., and Ackerman, T. P.: Comparison of Moderate Resolution Imaging Spectroradiometer ocean aerosol retrievals with ship – based Sun photometer measurements from the Around the Americas expedition, J. Geophys. Res., 116, doi:10.1029/2010JD015440, 2011. 3767

Anderson, T. L., Charlson, R. J., Winker, D. M., Ogren, J. A., and Holmen, K.: Mesoscale Variations of Tropospheric Aerosols, J. Atmos. Sci., 60, 119–136, 2003. 3773

Bréon, F.-M., Vermeulen, A., and Descloitres, J.: An evaluation of satellite aerosol products against sunphotometer measurements, Remote Sens. Environ., 115, 3102–3111, doi:10.1016/j.rse.2011.06.017, 2011. 3767, 3772

Eck, T. F., Holben, B. N., Reid, J. S., Dubovik, O., Smirnov, A., Neill, N. T. O., Slutsker, I., and Kinne, S.: Wavelength dependence of optical depth of biomass burning, urban and desert dust aerosols, J. Geophys. Res., 104, 31333–31349, 1999. 3770

Holben, B. N., Eck, T. F., Slutsker, I., Tanre, D., Buis, J. P., Setzer, A., Vermote, E., Reagan, J. A., Kaufman, Y. J., Nakajima, T., Lavenu, F., Jankowiak, I., and Smirnov, A.: AERONET – A Federated Instrument Network and Data Archive for Aerosol Characterization, Remote Sens. Environ., 66, 1–16, 1998. 3770

Huang, J., Hsu, N. C., Tsay, S.-C., Jeong, M.-J., Holben, B. N., Berkoff, T. A., and Welton, E. J.: Susceptibility of aerosol optical thickness retrievals to thin cirrus contamination during the BASE-ASIA campaign, J. Geophys. Res., 116, D08214, doi:10.1029/2010JD014910, 2011. 3770

AMTD
6, 3765–3818, 2013

Hyer, E. J., Reid, J. S., and Zhang, J.: An over-land aerosol optical depth data set for data assimilation by filtering, correction, and aggregation of MODIS Collection 5 optical depth retrievals, Atmos. Meas. Tech., 4, 379–408, doi:10.5194/amt-4-379-2011, 2011. 3768

Ichoku, C., Chu, D. A., Mattoo, S., Kaufman, Y. J., Remer, L. A., Tanre, D., Slutsker, I., and Holben, B. N.: A spatio-temporal approach for global validation and analysis of MODIS aerosol products, Geophys. Res. Lett., 29, MOD1.1–MOD1.4, doi:10.1029/2001GL013206, 2002. 3767, 3772

Ichoku, C., Remer, L., and Eck, T.: Quantitative evaluation and intercomparison of morning and afternoon Moderate Resolution Imaging Spectroradiometer (MODIS) aerosol measurements from Terra and Aqua, J. Geophys. Res., 110, D10S03, doi:10.1029/2004JD004987, 2005a. 3767, 3775

Ichoku, C., Remer, L., and Eck, T.: Correction to "Quantitative evaluation and intercomparison of morning and afternoon Moderate Resolution Imaging Spectroradiometer (MODIS) aerosol measurements from Terra and Aqua?", J. Geophys. Res., 110, D10S99, doi:10.1029/2005JD005897, 2005b. 3778

Kalnay, E., Kanamitsu, M., Kistler, R., Collins, W., Deaven, D., Gandin, L., Iredell, M., Saha, S., White, G., Woolen, J., Zhu, Y., Chelliah, M., Ebisuzaki, W., Higgins, W., Janowiak, J., Mo, K. C., Ropelewski, C., Wang, J., Leetmaa, A., Reynolds, R., Jenne, R., and Joseph, D.: The NCEP/NCAR 40-year reanalysis project, B. Am. Meteorol. Soc., 77, 437–471, 1996. 3771

Kovacs, T.: Comparing MODIS and AERONET aerosol optical depth at varying separation distances to assess ground-based validation strategies for spaceborne lidar, J. Geophys. Res., 111, doi:10.1029/2006JD007349, 2006. 3773

Liu, H. and Pinker, R. T.: Radiative fluxes from satellites : Focus on aerosols, J. Geophys. Res., 113, D08208, doi:10.1029/2007JD008736, 2008. 3767, 3771

Mishchenko, M. I., Geogdzhayev, I. V., Liu, L., Lacis, A. a., Cairns, B., and Travis, L. D.: Erratum to "Toward unified satellite climatology of aerosol properties: What do fully compatible MODIS and MISR aerosol pixels tell us?" [J. Quant. Spectrosc. Ra., 110, 402–408, 2009], J. Quant. Spectrosc. Ra., 110, 1962–1963, doi:10.1016/j.jqsrt.2009.05.015, 2009. 3767, 3775

Mishchenko, M. I., Liu, L., Geogdzhayev, I. V., Travis, L. D., Cairns, B., and Lacis, A. A.: Toward unified satellite climatology of aerosol properties, J. Quantit. Spectrosc. Ra., 111, 540–552, doi:10.1016/j.jqsrt.2009.11.003, 2010. 3767, 3770

AMTD
6, 3765–3818, 2013

Remer, L. A., Tanre, D., Kaufman, Y. J., Ichoku, C., Mattoo, S., Levy, R., Chu, D. A., Holben, B., Dubovik, O., Smirnov, A., Martins, J. V., Li, R., and Ahmad, Z.: Validation of MODIS aerosol retrieval over ocean, Geophys. Res. Lett., 29, 2–5, 2002. 3767

Remer, L., Kaufman, Y., Tanre, D., Mattoo, S., Chu, D., Martins, J., Li, R.-R., Ichoku, C., Levy, R., Kleidman, R., Eck, T., Vermote, E., and Holben, B.: The MODIS Aerosol Algorithm, Products, and Validation, J. Atmos. Sci., 62, 947–973, 2005. 3767, 3770, 3785, 3816

Remer, L. A., Kleidman, R. G., Levy, R. C., Kaufman, Y. J., Tanré, D., Mattoo, S., Martins, J. V., Ichoku, C., Koren, I., Yu, H., and Holben, B. N.: Global aerosol climatology from the MODIS satellite sensors, J. Geophys. Res., 113, D14S07, doi:10.1029/2007JD009661, 2008. 3767

Santese, M., De Tomasi, F., and Perrone, M. R.: AERONET versus MODIS aerosol parameters at different spatial resolutions over southeast Italy, J. Geophys. Res., 112, D10214, doi:10.1029/2006JD007742, 2007. 3773

Schmid, B., Michalsky, J., Halthore, R., Beauharnois, M., Harnson, L., Livingston, J., Russell, P., Holben, B., Eck, T., and Smirnov, A.: Comparison of Aerosol Optical Depth from Four Solar Radiometers During the Fall 1997 ARM Intensive Observation Period, Geophys. Res. Lett., 26, 2725–2728, 1999. 3770

Schutgens, N., Nakata, M., and Nakajima, T.: Estimating Aerosol Emissions by Assimilating Remote Sensing Observations into a Global Transport Model, Remote Sensing, 4, 3528–3543, doi:10.3390/rs4113528, 2012. 3787

Shi, Y., Zhang, J., Reid, J. S., Holben, B., Hyer, E. J., and Curtis, C.: An analysis of the collection 5 MODIS over-ocean aerosol optical depth product for its implication in aerosol assimilation, Atmos. Chem. Phys., 11, 557–565, doi:10.5194/acp-11-557-2011, 2011. 3767, 3768, 3771, 3772, 3775, 3776, 3779, 3785, 3786, 3787, 3796, 3816

Smirnov, A., Holben, B. N., Giles, D. M., Slutsker, I., O'Neill, N. T., Eck, T. F., Macke, A., Croot, P., Courcoux, Y., Sakerin, S. M., Smyth, T. J., Zielinski, T., Zibordi, G., Goes, J. I., Harvey, M. J., Quinn, P. K., Nelson, N. B., Radionov, V. F., Duarte, C. M., Losno, R., Sciare, J., Voss, K. J., Kinne, S., Nalli, N. R., Joseph, E., Krishna Moorthy, K., Covert, D. S., Gulev, S. K., Milinevsky, G., Larouche, P., Belanger, S., Horne, E., Chin, M., Remer, L. A., Kahn, R. A., Reid, J. S., Schulz, M., Heald, C. L., Zhang, J., Lapina, K., Kleidman, R. G., Griesfeller, J., Gaitley, B. J., Tan, Q., and Diehl, T. L.: Maritime aerosol network as a component of AERONET – first results and comparison with global aerosol models and satellite retrievals, Atmos. Meas. Tech., 4, 583–597, doi:10.5194/amt-4-583-2011, 2011. 3767, 3771

AMTD
6, 3765–3818, 2013

Tanre, D., Kaufman, Y. J., Herman, M., and Mattoo, S.: Remote sensing of aerosol properties over ocean using the MODIS/EOS spectral radiances, J. Geophys. Res., 102, 16971–16988, 1997. 3767

Zhang, J. and Reid, J. S.: MODIS aerosol product analysis for data assimilation: Assessment of over-ocean level 2 aerosol optical thickness retrievals, J. Geophys. Res., 111, D22207, doi:10.1029/2005JD006898, 2006. 3767, 3768, 3771, 3772, 3775, 3776, 3779, 3785, 3786, 3787, 3796, 3816

AMTD
6, 3765–3818, 2013

Table 1. Comparison between three relevant studies

	Zhang and Reid (2006)	Shi et al. (2011)	This paper
Period	Aqua: Sep 2004–Aug 2005 Terra: 2004	Aqua: 2002–2008 Terra: 2000–2008	Aqua: 2003–2009 Terra: 2003–2009
Collection	4	5	5
MODIS	AOT at 470, 550 and 860 nm	AOT at 550 nm	AOT at 550 nm AE at 860/470 nm
AERONET	lvl 1.5	lvl 2.0	lvl 2.0
Marine AERONET	no	no	yes
co-location	0.3°, 20^m	0.3°, 30^m	50 km, 30^m
Windspeeds	NOGAPS	NOGAPS	NCEP-DOE– II
Sample	dependent	dependent	independent

AMTD
6, 3765–3818, 2013

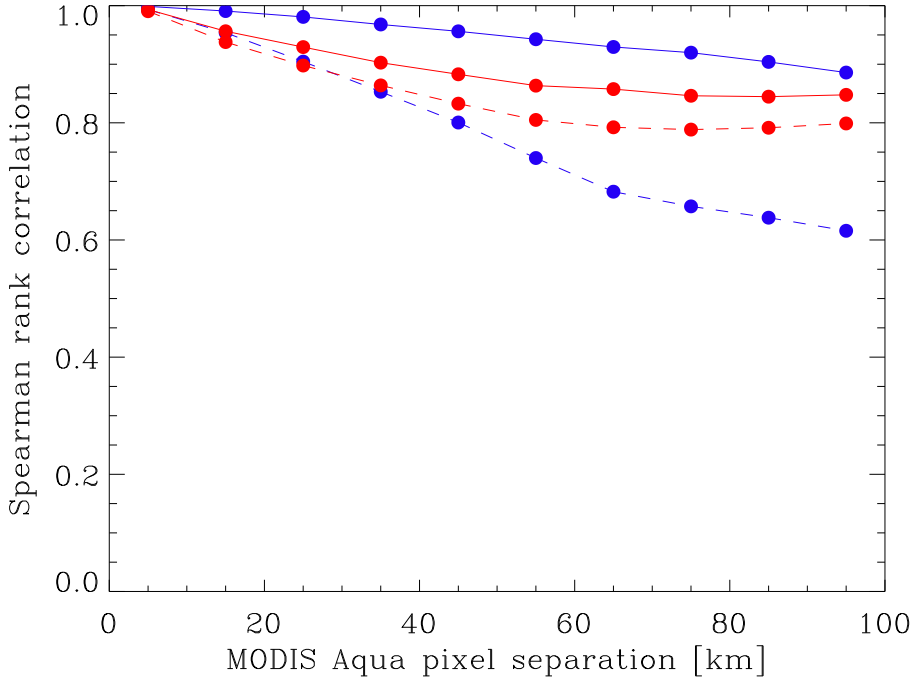

Fig. 1. Spatial correlations among MODIS observations (solid blue: AOT, solid red: AE) or their errors (dashed) as a function of separation.

AMTD
6, 3765–3818, 2013

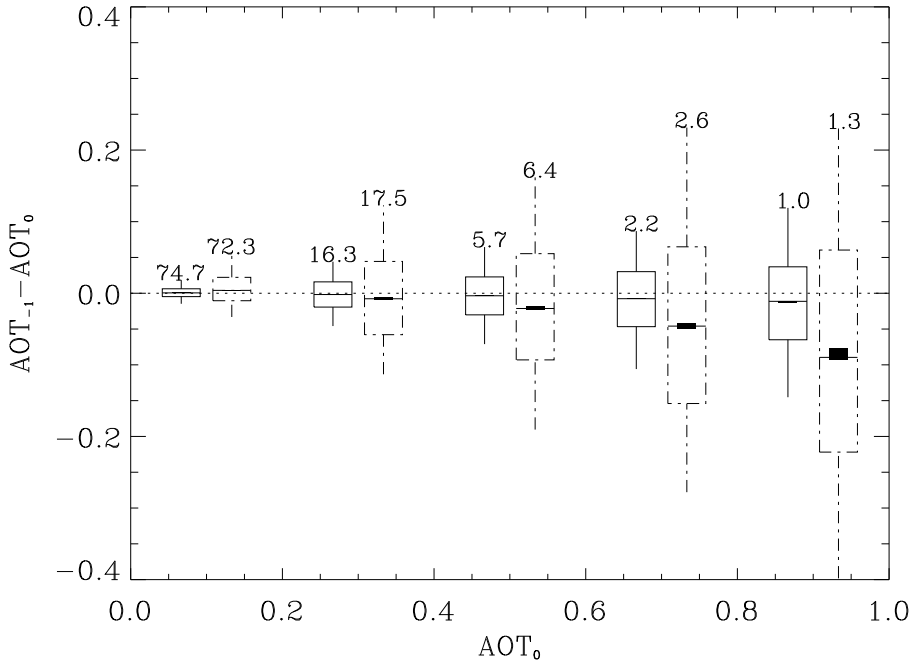

Fig. 2. Apparent biases in AOT differences between AERONET observations at different times: for one 1 h separation (solid) or 6 h separation (dash-dot).

AMTD
6, 3765–3818, 2013

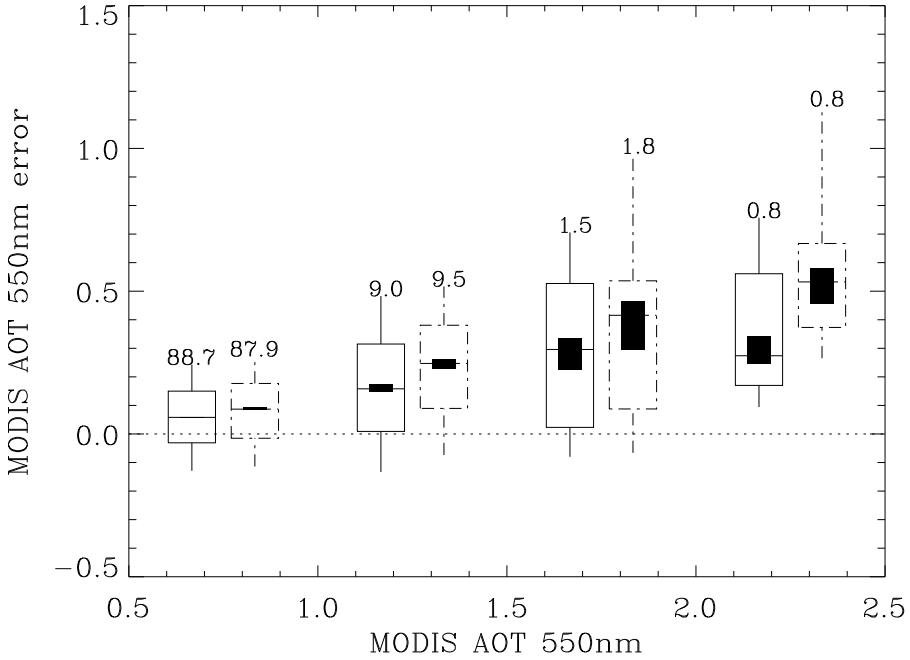

Fig. 3. MODIS AOT error statistics as a function of MODIS AOT for the full sample (solid line) of observations or an independent sub-sample (dash-dotted line). The box-whisker plots are offset from the bin centers to show the two distributions side by side.

AMTD
6, 3765–3818, 2013

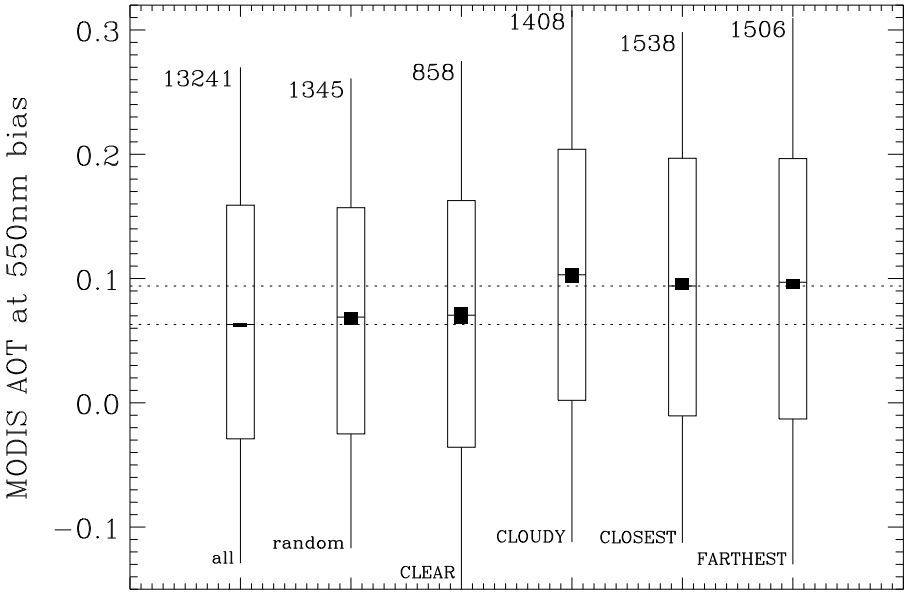

Fig. 4. MODIS AOT error statistics for $0.5 \leq \tau \leq 2.5$ depending on different sampling of our data.

AMTD
6, 3765–3818, 2013

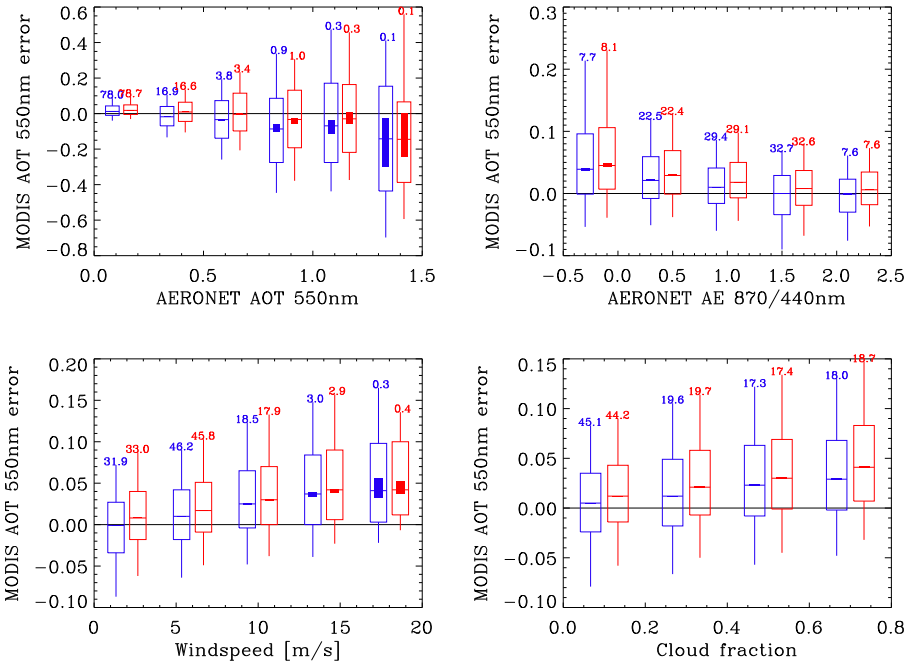

Fig. 5. MODIS AOT error statistics as a function of AERONET AOT, AERONET AE, NCEP-DOE-II windspeed and MODIS cloud fraction (blue: Aqua; red: Terra). The box-whisker plots are offset from these bin centers to show the two distributions side by side.

AMTD
6, 3765–3818, 2013

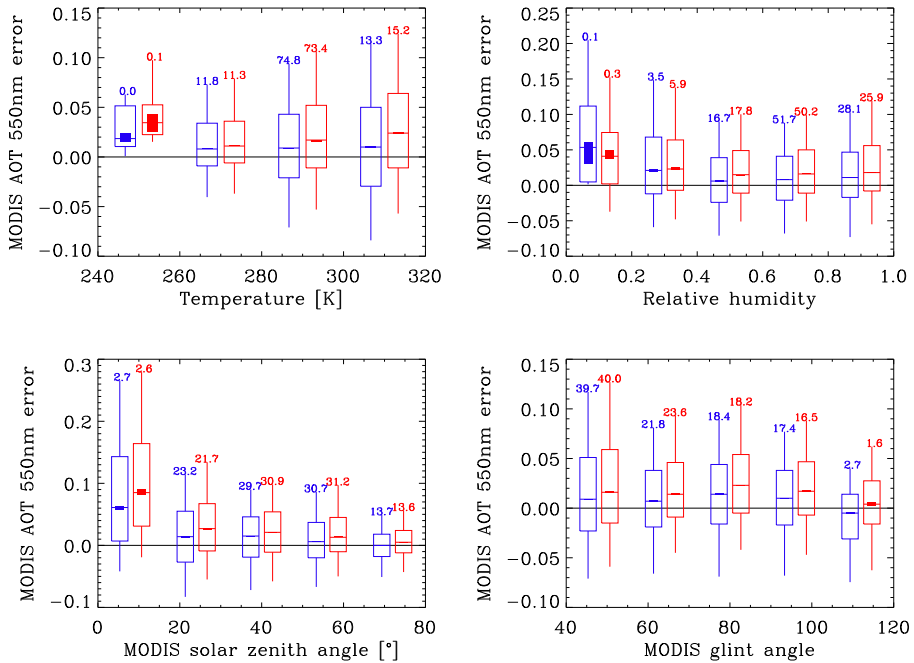

Fig. 6. MODIS AOT error statistics as a function of NCEP-DOE-II temperature (2 m) or relative humidity (2 m), MODIS scattering or glint angle (blue: Aqua; red: Terra). The box-whisker plots are offset from these bin centers to show the two distributions side by side.

AMTD
6, 3765–3818, 2013

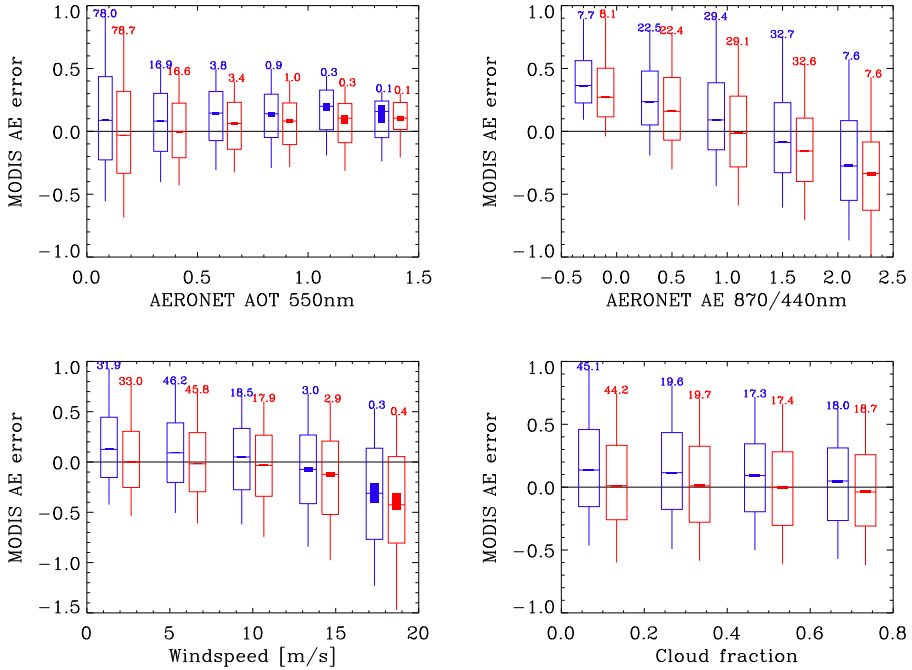

Fig. 7. MODIS AE error statistics as a function of AERONET AOT, AERONET AE, NCEP-DOE-II windspeed and MODIS cloud fraction (blue: Aqua; red: Terra). The box-whisker plots are offset from these bin centers to show the two distributions side by side.

AMTD
6, 3765–3818, 2013

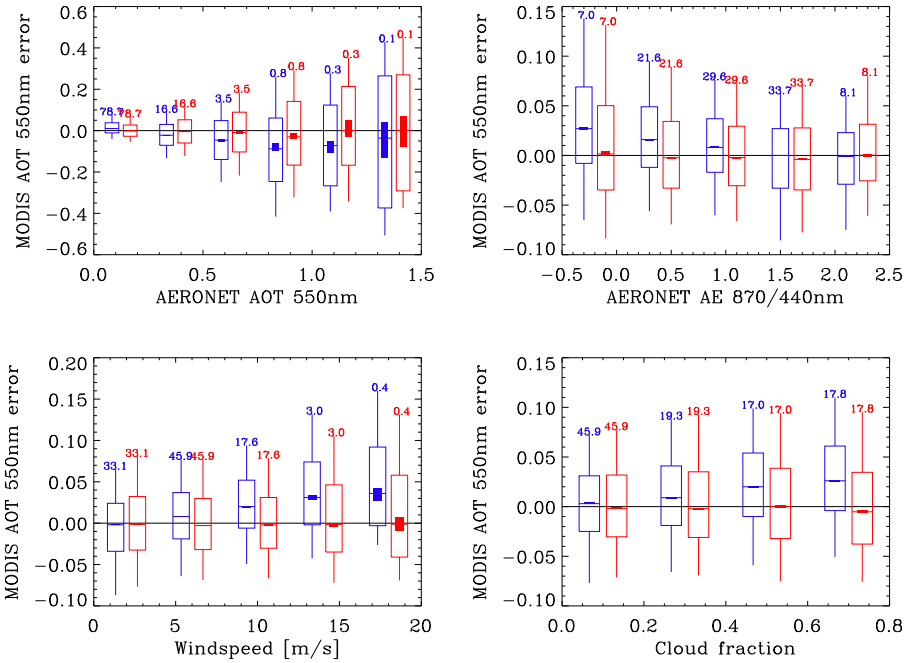

Fig. 8. MODIS Aqua AOT error statistics as a function of AERONET AOT, AERONET AE, NCEP-DOE-II windspeed and MODIS cloud fraction for the original (blue) and the corrected AOT (red). The box-whisker plots are offset from these bin centers to show the two distributions side by side.

AMTD
6, 3765–3818, 2013

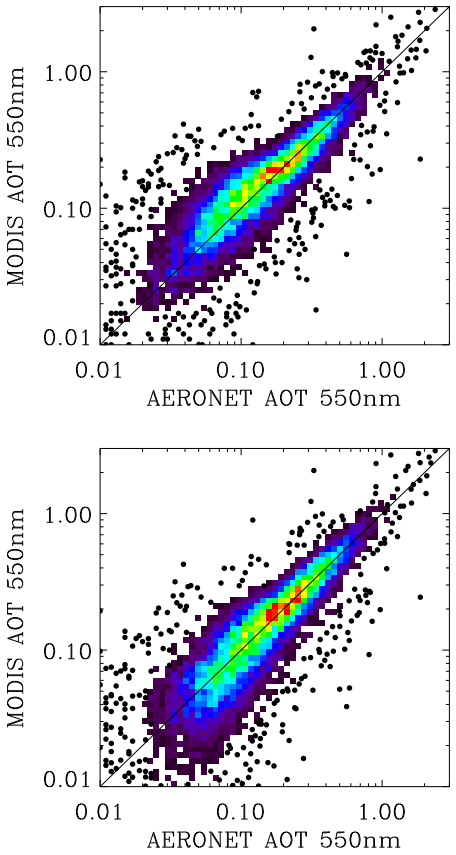

Fig. 9. Density plots of MODIS Aqua AOT vs. AERONET AOT for the original (top) and corrected (bottom) samples.

AMTD
6, 3765–3818, 2013

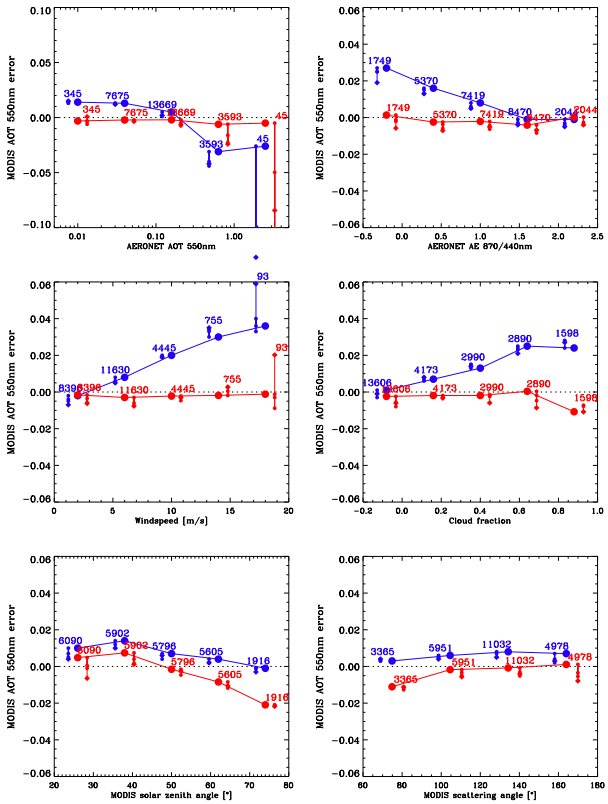

Fig. 10. Biases in Aqua AOT for different subsamples, for both the original (blue) and corrected (red) observations. The dots along the vertical bars represent the biases for three subsamples (closest, random or farthest)). The diamond represents the bias for the full dataset. The fatter dots, connected by lines, represent the biases for the sub-sample that was used to construct the correction algorithm (closest).

AMTD
6, 3765–3818, 2013

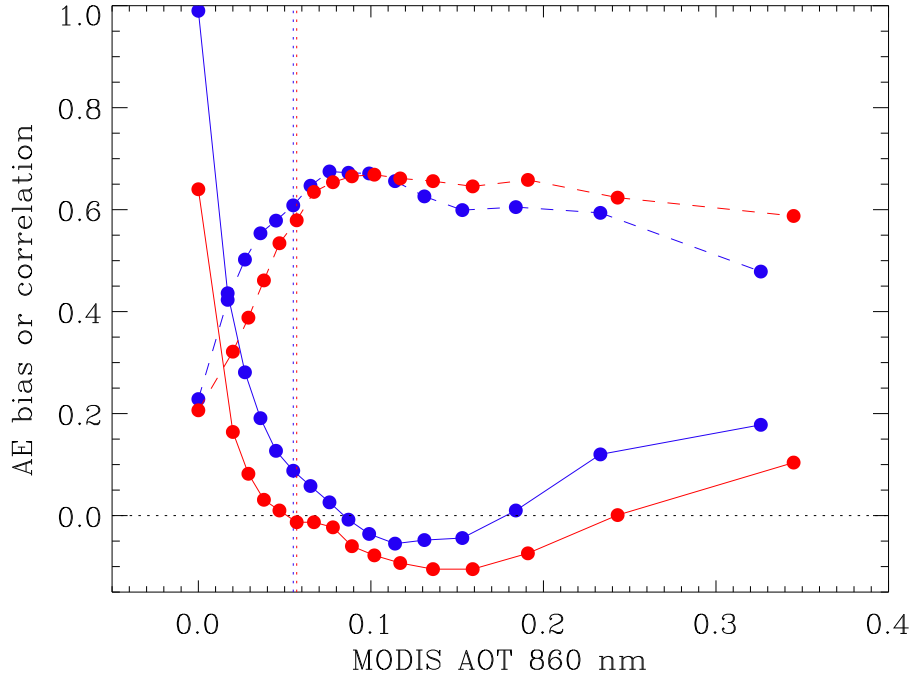

Fig. 11. Bias and correlation of MODIS AE vs AERONET AEfor Aqua (blue) and Terra (red). Bias and correlation were calculated for MODIS AOT at 860 bins. The horizontal axis shows the lower AOT value of each bin. Bins contain equal numbers of observations (per bin 6.25% of all observations). The vertical lines are the chosen thresholds.

AMTD
6, 3765–3818, 2013

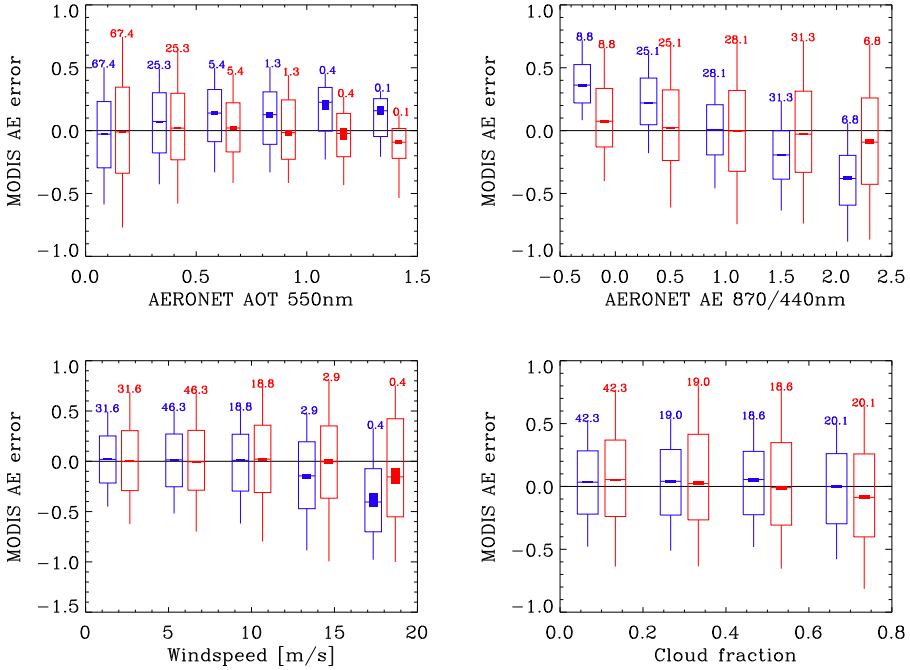

Fig. 12. MODIS Aqua error statistics as a function of AERONET AOT, AERONET AE, NCEP-DOE-II windspeed and MODIS cloud fraction for the original (blue) and the corrected AE (red). The box-whisker plots are offset from these bin centers to show the two distributions side by side.

AMTD
6, 3765–3818, 2013

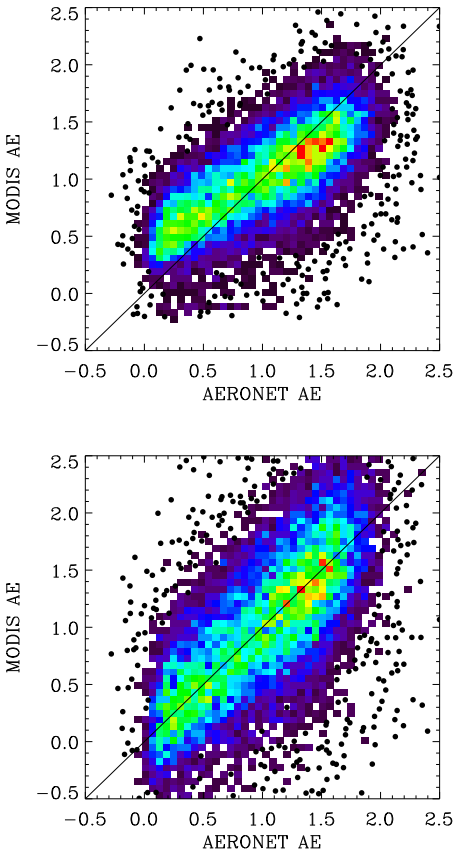

Fig. 13. ensity plots of MODIS Aqua AE vs. AERONETAE for the original (top) and corrected (bottom) samples.

AMTD
6, 3765–3818, 2013

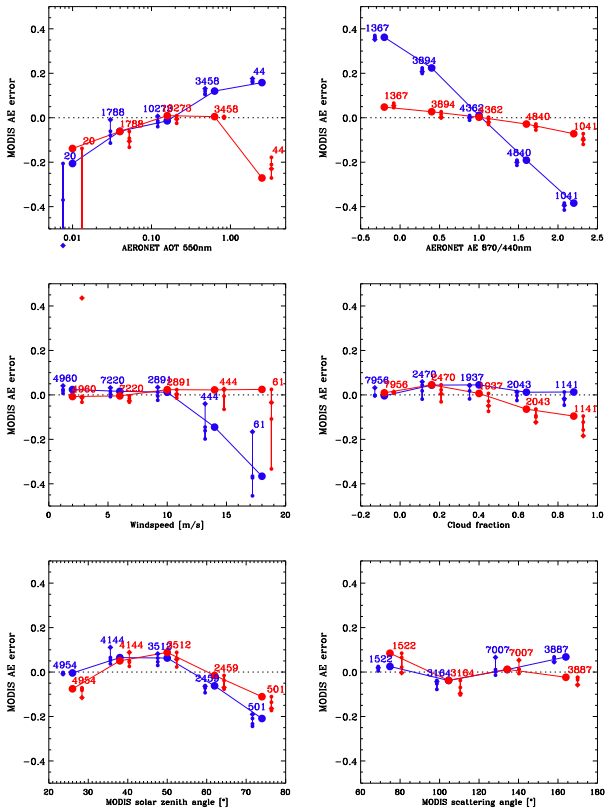

Fig. 14. Biases in Aqua AE for different subsamples, for both the original (blue) and corrected (red) observations. The dots along the vertical bars represent the biases for three subsamples (closest, random and farthest). The diamond represents the bias for the full dataset. The fatter dots, connected by lines, represent the biases for the sub-sample that was used to construct the correction algorithm (closest).

AMTD
6, 3765–3818, 2013

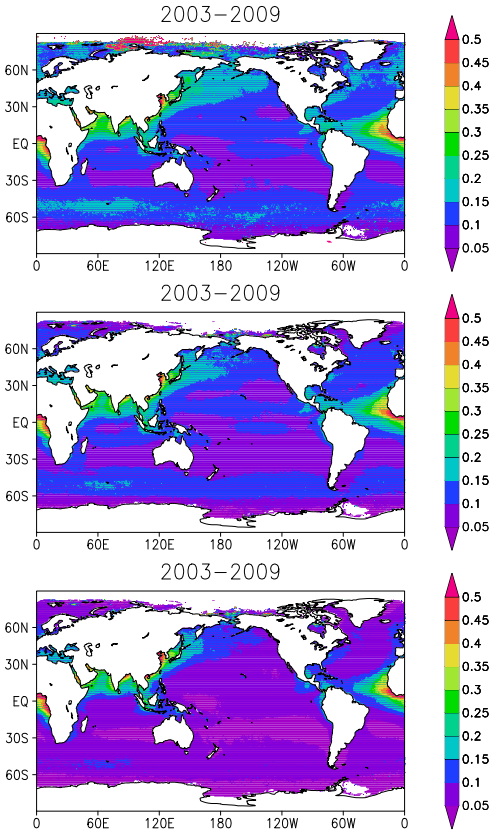

Fig. 15. Multi-year averages (2003-2009) of MODIS Aqua AOT. The top panel shows the original MODIS Coll. 5 lvl 2 product. The middle panel shows the screened product and the bottom panel shows the corrected product.

AMTD
6, 3765–3818, 2013

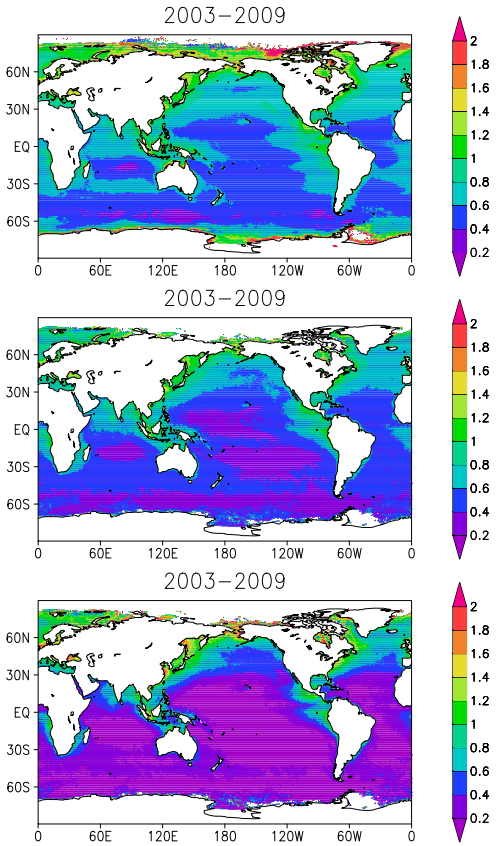

Fig. 16. Multi-year averages (2003-2009) of MODIS Aqua AE. The top panel shows the original MODIS Coll. 5 lvl 2 product. The middle panel shows the screened product and the bottom panel shows the corrected product.

AMTD
6, 3765–3818, 2013

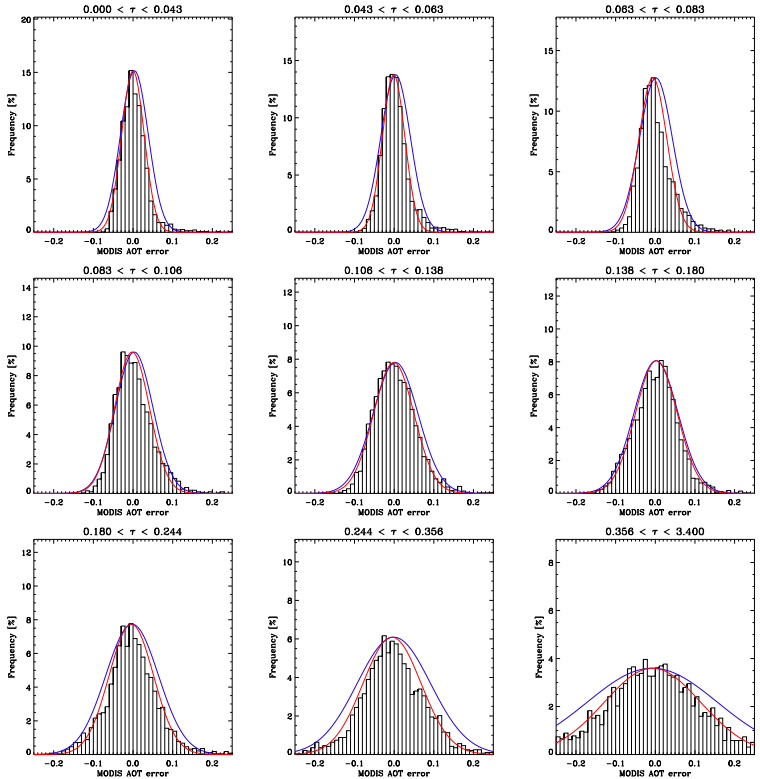

Fig. 17. Random Aqua AOT errors distributions for the corrected observations per AERONET AOT bin. Also shown are two Gaussian distributions to model these random errors, based on the standard deviation (blue) or an interquantile range (red).

AMTD
6, 3765–3818, 2013

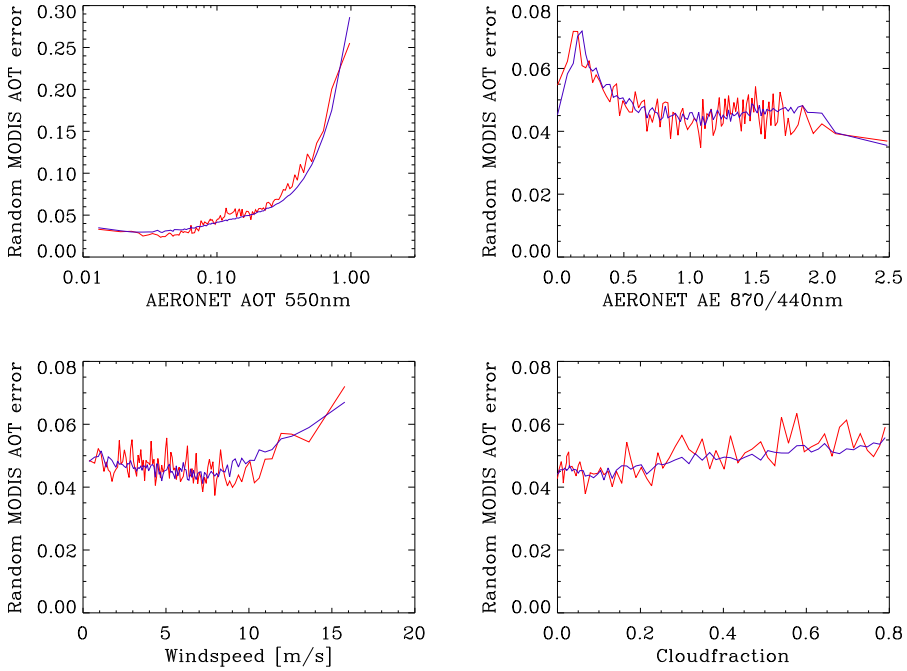

Fig. 18. Random Aqua AOT errors in the corrected observatons. In red, the error estimated from binned observations, in blue our error model.

AMTD
6, 3765–3818, 2013

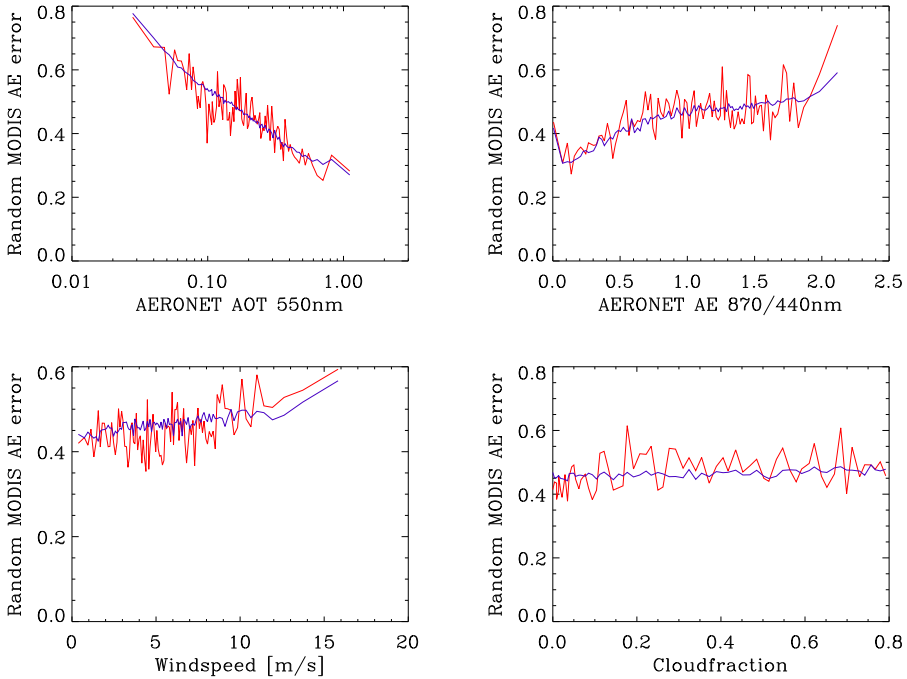

Fig. 19. Random Aqua AE errors in the corrected observatons. In red, the error estimated from binned observations, in blue our error model.

AMTD
6, 3765–3818, 2013

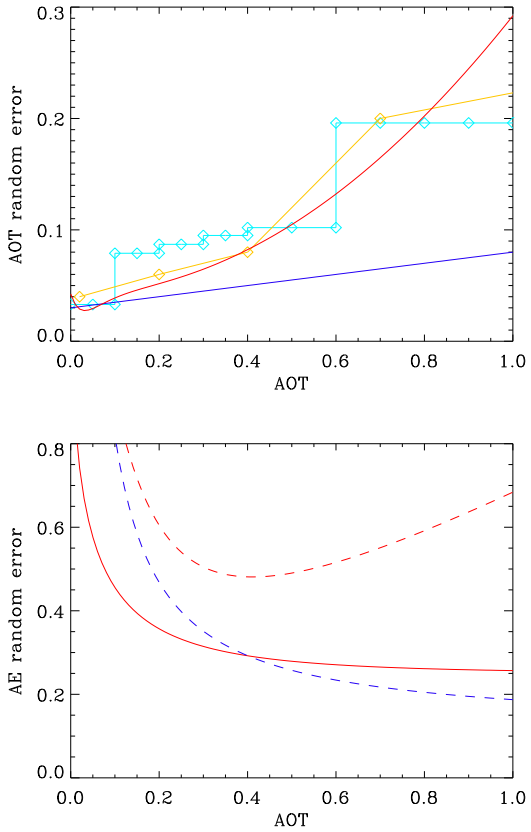

Fig. 20. Comparison of random error estimates for MODIS Aqua AOT and AE. In the top panel, AOT random errors estimated by (Remer et al., 2005) (blue), (Zhang and Reid, 2006) (light blue), (Shi et al., 2011) (orange) and this study (red). In the bottom panel, AE random errors estimated in this study (solid red), or from a prediction based on this study's AOT random errors (dashed red) or (Remer et al., 2005) AOT random errors (dashed blue).

AMTD
6, 3765–3818, 2013

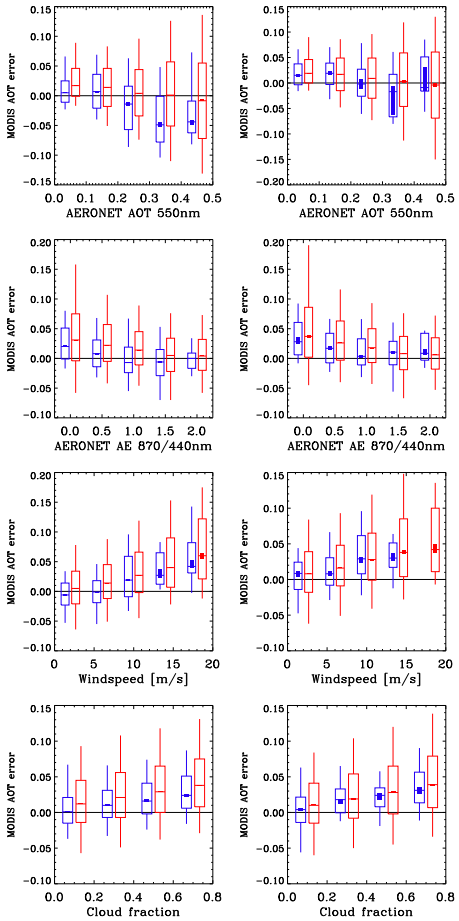

Fig. 21. Terra AOT error statistics from comparison against Marine AERONET (blue) or AERONET for either the full dataset (left) or an independent sample (right). For the independent samples, Marine AERONET and AERONET data yield very a similar picture.

AMTD
6, 3765–3818, 2013

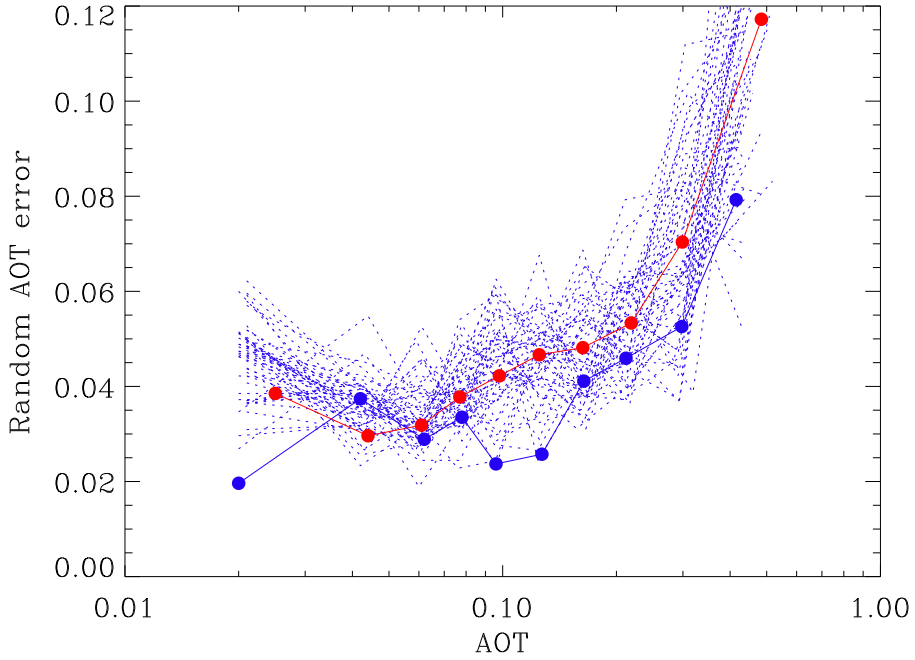

Fig. 22. Terra random AOT errors estimated from Marine AERONET (blue) or AERONET (red). The blue dotted lines are random error estimates from a sub-sample of AERONET sampled to mimick Marine AERONET properties.

AMTD
6, 3765–3818, 2013